Mesh material low pass filters for millimeter wave applications: is the square capacitive shape optimal?

Jonathan A. Thompson[a,*], **Giampaolo Pisano**[a], **Carole Tucker**[a]
[a]School of Physics and Astronomy, Cardiff University, The Parade, Cardiff UK, CF24 3AA

Abstract. The use of mesh filters for millimeter wave applications using capacitive and inductive grids is well known and they are widely used in cosmic microwave background instrumentation. We report here on an investigation into whether the capacitive square shape typically used in low pass filter designs, could be improved upon. The micro-genetic algorithm and the finite differences, time domain, electromagnetic modelling method were used to look for shape variations to the standard square shape. Any shape changes discovered were then analysed to establish which variations had the most effect. We shall show that improvements found using pixelated patterns evolved by the genetic algorithm were somewhat mixed.

Keywords: millimeter waves, FDTD, genetic algorithm, mesh filter.

*Jonathan A. Thompson, thompsonja3@cardiff.ac.uk

1 Introduction

Filters for millimeter electromagnetic waves are an essential part of many radio astronomical instruments and their implementation using metallic mesh grids is becoming common place. Their design, however, can still be a somewhat involved process and tends to be restricted to a small number of well-known patterns, namely square plates (for capacitive grids) and square holes (inductive grids).

The study reported here set out to discover if there were any improvements that could be made to a capacitive mesh made from square patches when used for low pass filters. The investigation procedure consisted of three stages; finding an initial conventional design, improving the design by varying the layer pattern and then decomposing the pattern changes. A genetic algorithm coupled to an electromagnetic modelling method was used in the first two stages.

The use of square patch and square hole metal meshes to construct low and high pass filters was first described by Ulrich.[1] Pisano et al[2] review many device types that have been implemented

using such meshes in millimetre wave astronomy instrumentation, while Ade et al[3] concentrates on filter applications. A combination of the square patch and hole (often referred to as a cross) has been used to produce a band pass response; Moallem and Sarabandi[4] and Wang et al[5] describe examples while Melo et al[6] reviews the history of its use and mentions other patterns that have been investigated. Split ring resonators have also been used in band pass and band stop filters, Navarro-Cia et al[7] and Kundu et al[8] are examples. Wu et al[9] investigate a fractal pattern to provide a similar response.

The use of a genetic algorithm as a search method was first described by Holland[10] and later by Goldberg.[11] The Micro-Genetic Algorithm (MGA), an improvement that does not require large numbers of candidate solutions to be evaluated, was proposed by Krishnakumar.[12] Ge and Esselle[13] described using the MGA and the finite differences, time domain (FDTD) modelling method to explore unconventional patterns for reflective surfaces. The patterns were constructed from 16x16 pixelated grids with four fold symmetry. Sui et at[14] use this technique to design and construct a frequency selective surface absorber and Thompson and Pisano[15] extended the method to find designs for millimeter wave transmission devices. Ranjan et al[16,17] use a binary wind driven optimisation algorithm with pixelated patterns to design frequency selective surfaces. Mohammed et al[18] compare a number of nature inspired optimisation algorithms, including the genetic algorithm, when applied to antenna design. Campbell et al[19] review the general field of numerical optimisation applied to electromagnetic device design.

The first stage of the investigation consisted of searching for low pass filter solutions using the genetic algorithm and the propagation matrix electromagnetic modelling method described by Orfanadis.[20] Admittance curves were computed for various sizes of conventional square capacitive plate in a standard unit cell. This information was used to derive admittance curves for the desired

unit cell and plate size by scaling and interpolation. The propagation matrix method used this information to rapidly model a solution and generate its transmittance and phase shift characteristics. In this way, large numbers of generations of possible solutions can be assessed in a short time to arrive at an initial low pass filter design using the MGA search algorithm.

In the second stage, this initial solution was used as a starting point for a further MGA search using the FDTD electromagnetic modelling method, described by Taflove and Hagness[21] and by Schneider.[22] The conventional square plates were converted into NxN pixelated panels, the value of N being chosen so as to represent the initial solution as closely as possible while still keeping the search space and FDTD model reasonably sized. The search then proceeds with the genetic algorithm varying the patterns away from the initial conventional square shapes, while keeping the unit cell and layer spacing fixed at the values found in stage 1. This stage is rather more processor intensive than the first stage and was undertaken on Cardiff University's Hawk compute cluster.

The NxN patterns resulting from stage 2 usually showed the basic outline of the starting shapes from stage 1 with a number of changes, for example, corners cut off, extra protrusions, holes etc. In the third stage, changes were identified and tested in isolation to establish their individual effects.

A number of constraints were applied to the designs produced by the first stage. They were restricted to 4 layers, two instances of each of two patterns arranged symmetrically. The sizes of the square shapes for the initial conventional designs were required to fit on the FDTD grid used for the second stage pattern search. The unit cell used on each layer was restricted to a simple set of ratios, 1:1, 2:1, to allow the designs to be easily modelled. Since possible improvements due to the layer patterns are being investigated, it does not matter that the initial designs are not necessarily optimal due to these constraints, any improvements found due to shape variation should still be applicable.

2 The Electromagnetic Modelling Methods

The propagation matrix method, used in stage 1, is described in detail by Orfanidis.[20] The method is a one-dimensional solution of Maxwell's equations, separating waves into forward and reverse components. Matrices were derived that represent waves travelling through dielectrics (propagation matrices) and across boundaries between different dielectrics (matching matrices). The treatment is easily extensible to cover the metallic meshes that are the subject of this study by using their complex admittance either from a formula, for example one those collected together by Lee et al,[23] or by using modelling tools to measure it, the approach taken here. Thompson and Pisano[15] provide a summary of the modelling method as implemented.

The second stage utilised FDTD, a three-dimensional modelling method that calculates the solutions to Maxwell's equations using second order finite differences. Good descriptions of the method are given by Taflove and Hagness[21] and Schneider.[22] The implementation used here is described in Thompson and Pisano[15] and was verified against Ansys HFSS.[24]

3 The Micro-Genetic Algorithm

The MGA used to perform the searches is described by Krishnakumar[12] and the implementation utilised here is a development of that described in Thompson and Pisano.[15] It proceeds as shown in Fig. 1.

To calculate the fitness of each individual, the results from the electromagnetic model are assessed against a fitness function. In this study, the transfer functions of two common low pass filter types, Butterworth and Chebyshev, were used. The area between the modelled curve and the fitness function was used as the measure of unfitness.

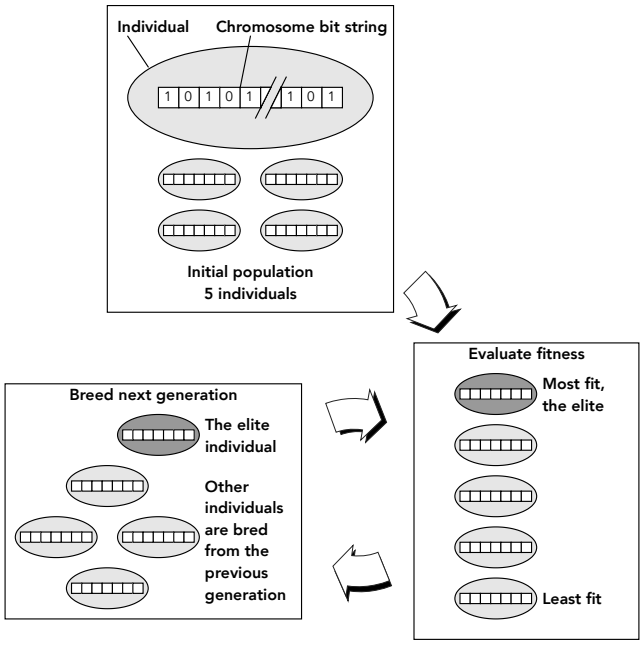

Fig 1 The micro-genetic algorithm. The starting point is an initial population of 5 individuals. Their chromosome bit strings are normally generated randomly, but in stage 2 of the methodology one of the individuals is initialized from the best solution of stage 1. The fitness of each individual is then assessed by running the electromagnetic model on the structure represented by its chromosome and comparing the results with the fitness function. The best individual is marked as the elite and is automatically included in the next generation. Four new members are then bred from the previous generation to bring the numbers back to 5. A check is performed to maintain the genetic diversity of the generation; if all the individuals have more than 95% of their chromosomes identical, the four bred individuals are replaced with completely new random individuals. The loop then continues with fitness evaluation.

The patterns used by the MGA to improve the fit of a solution to the desired transfer function were N by N (N is always even), four-fold symmetric, pixelated plates. The 16 by 16 pixel plate was used by Ge and Esselle[1] in their study. Here the resolution of the plate is chosen such that the starting point for stage 2 can be reasonably accurately represented. The disadvantage of higher resolution plates is that they increase the size of the solution space being searched. To maintain the four-fold symmetry that all the filter designs described here require, only one triangle of a plate is actually specified, as shown in Fig. 2.

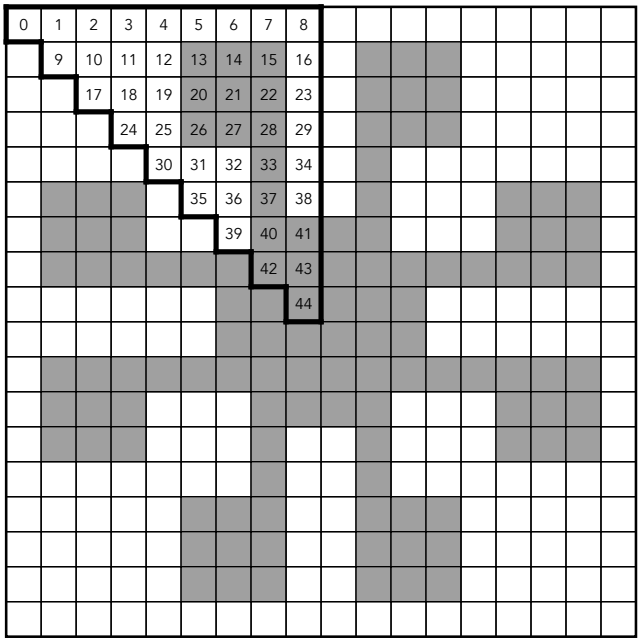

Fig 2 A pixelated plate and its binary encoding. As described by Ge and Esselle[13] and reiterated in Thompson and Pisano,[15] a four-fold pixelated NxN plate can be represented by the binary code covering one triangle of the plate as shown in this example of an 18x18 plate. The numbers in the pixels indicate the bit number in the gene encoding.

4 Results

The methodology outlined in the previous sections was used to investigate two low pass filter designs; a seventh order Chebyshev and a fifth order Butterworth.

4.1 Seventh order Chebyshev low pass filter

A seventh order low pass Chebyshev filter with a pass-band ripple of 0.5dB was specified as the fitness function for the first investigation. The conventional squares solution found by stage 1 is shown in Fig. 3. The stage 2 search was then initialised with this information and the layer patterns found are shown in Fig. 4. The transmittance curves are shown in Fig. 5, showing how the pattern changes made by stage 2 have brought the response closer to the ideal.

The losses incurred by the signal passing through the filter were estimated by measuring both the transmittance and the reflectance. These are shown in Fig. 6. The losses for both the capacitive

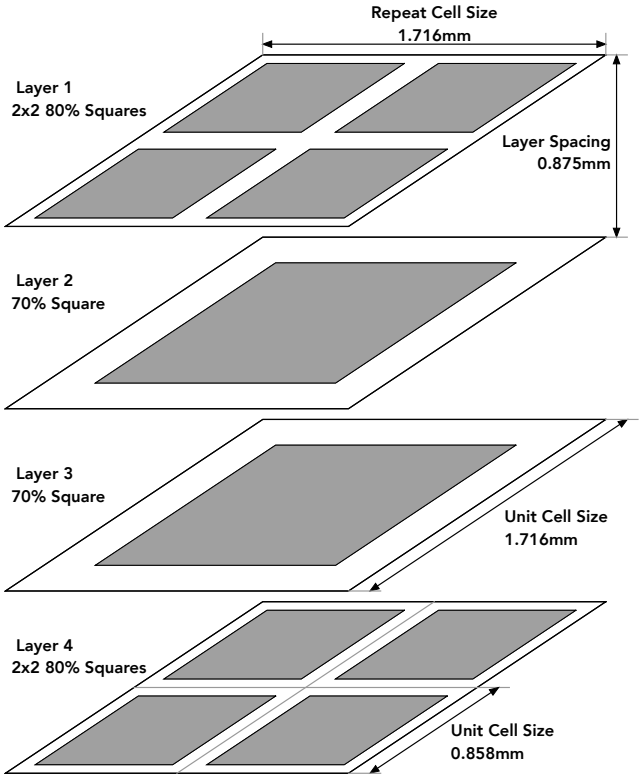

Fig 3 The best solution from stage 1 for the seventh order Chebyshev low pass filter example. It consists of two layers repeated in reverse order with a repeat cell size of 1.716mm and a layer spacing of 0.875mm. Layers 1 and 4 consist of a 2x2 layout of 80% squares each in a unit cell of 0.858mm. Layers 2 and 3 are single 70% squares in a unit cell of 1.716mm covering the entire repeat cell.

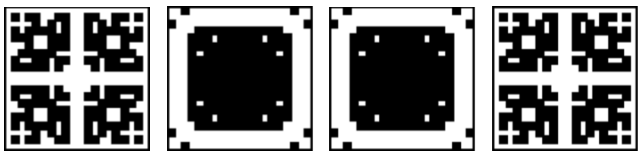

Fig 4 The best solution from stage 2 for the seventh order Chebyshev low pass filter example. These are the 4-fold 20x20 binary patterns settled on for the four layers.

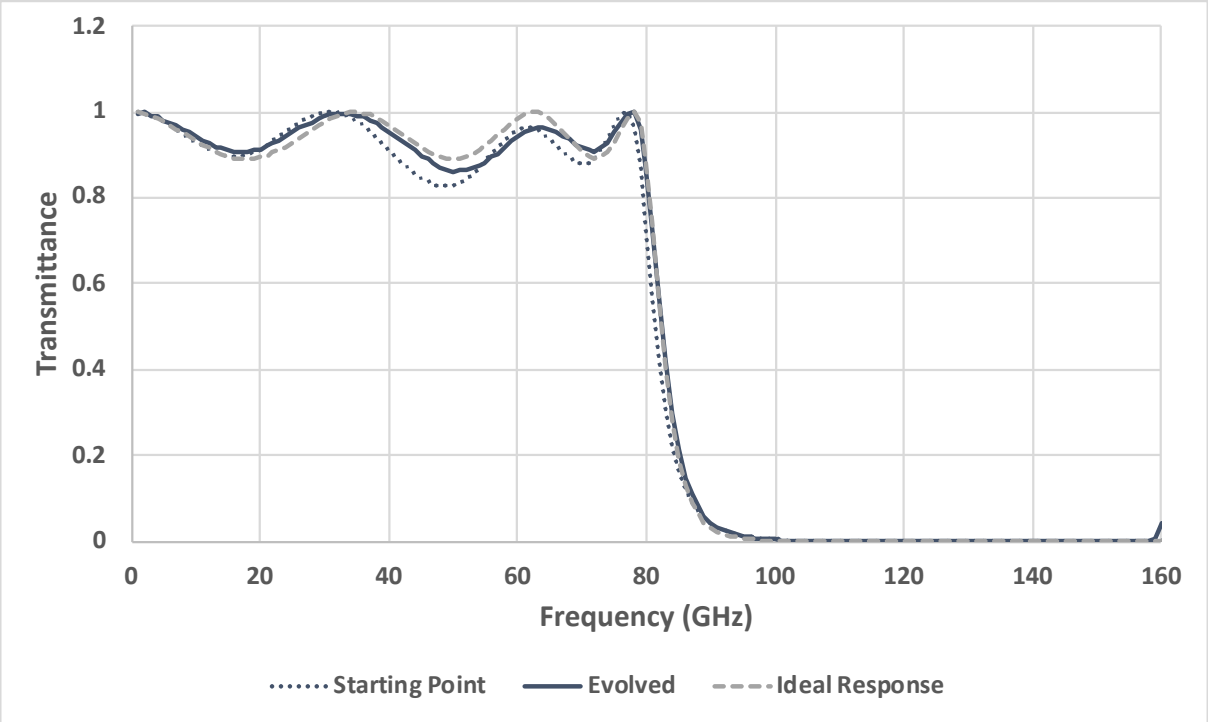

Fig 5 The transmittance curves of the starting point (the best solution from stage 1), the best evolved solution from stage 2 and the ideal filter response. It can be seen that the plate pattern changes from the stage 2 evolution have caused the transmittance characteristic to move closer to the target; most significantly, the pass-band ripple has been reduced.

squares pattern produced by stage 1 and the binary pattern produced by stage 2 are pretty much identical within the passband of the filter and below the diffraction limit, within the accuracy limits of the FDTD modelling technique. The losses of the evolved design do increase in the stop band.

The effect of the various changes made by the genetic algorithm were then investigated in stage 3. An error value was calculated for the stage 2 result by measuring the area between its transmittance curve and the target curve. Pattern features introduced by the genetic algorithm were then removed one by one and the FDTD model run to allow the calculation of an error for each case. The effect of each pattern feature could then be assessed. All the results of this are shown in Fig. 7. The conventional capacitive squares solution produced by stage one, returned an error of 3.19 (the units are GHz, the transmittance being a power ratio). The evolved solution of stage 2 showed an error of 1.68. The evolved solution reduced the error by 47%, most of the change

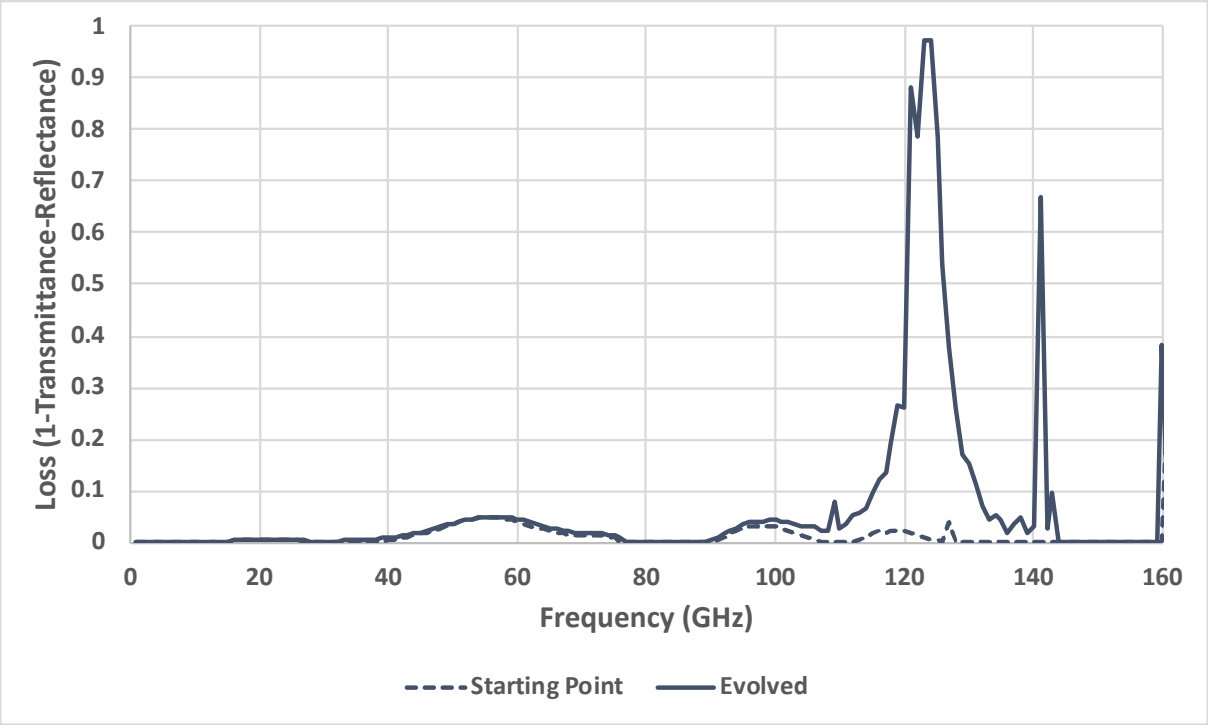

Fig 6 The losses of the starting point (the best solution from stage 1) and the best evolved solution from stage 2 for the Chebyshev filter. The losses of the two solutions are minimal and similar within the passband. In the stop band, however, the evolved solution showed significant loss around 125GHz. The diffraction limit is at 160GHz.

coming in the ripple in the passband.

4.2 Butterworth low pass filter

For the second example, a fifth order low pass Butterworth filter was specified as the fitness function. To obtain a reasonable Butterworth response, it proved necessary to reduce the upper limit to 125GHz, thus easing the requirements on the diffraction zone. The result of stage 1 is shown in Fig. 8. The stage 2 search was initialised with this result, the layer patterns found are shown in Fig. 9 and the transmittance curves of the stage 1 solution, stage 2 solution and the ideal are shown in Fig. 10.

Using the same error estimating method as for the Chebyshev case, an error reduction of just 8% is achieved by the evolved design over the conventional squares. However, unlike with the

Description	Layers 1&4	Layers 2&3	Comments
Stage 1 result Error: 3.19			The conventional square capacitive plates result
Stage 2 result Error: 1.68 Improvement: 47%			The solution evolved from the conventional result
Layers 2&3 corner dots Error: 1.90 Improvement: 40%			The dots only make a small difference to the error
Layers 2&3 plate holes Error: 1.71 Improvement: 46%			These plate holes make even less difference
Layers 2&3 plate corners not cut off Error: 2.74 Improvement: 14%			This change makes the biggest difference of all the changes made to layers 2&3
Layers 1&4 plate center holes Error: 1.84 Improvement: 42%			The holes in the center of the layer 1&4 plates make only a small difference
Layers 1&4 middle corners Error: 1.97 Improvement: 38%			Only a small difference made by this feature
Layers 1&4 outer corners Error: 2.20 Improvement: 31%			The rounding of the outer corners of layers 1&4 do make a difference

Fig 7 Fitness factors were calculated for the result of stage 2 and for patterns with various stage 2 changes removed. The conclusion is that the corners of layers 2&3 and the outer corners of layers 1&4 make the most difference. The other changes appear to make only a marginal difference.

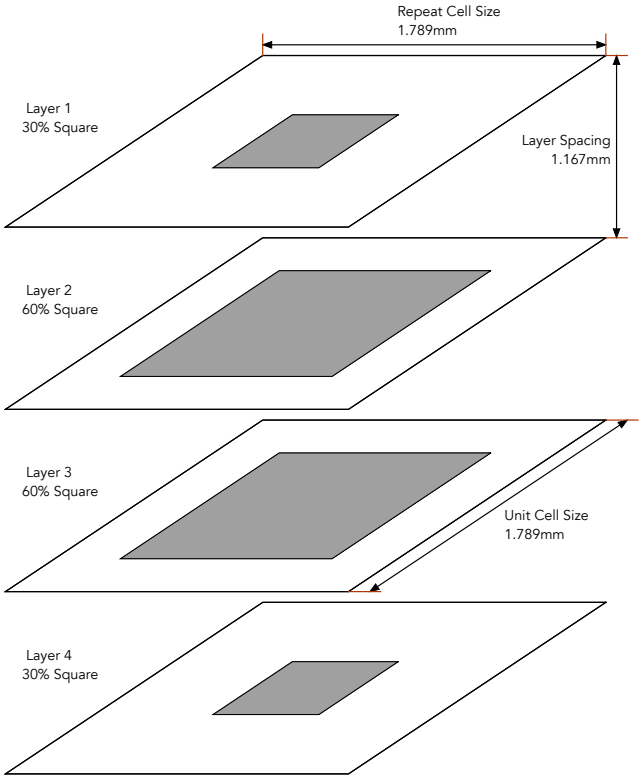

Fig 8 The best solution from stage 1 for the fifth order Butterworth low pass filter example. It consists of two layers repeated in reverse order with a repeat cell size of 1.789mm and a layer spacing of 1.167mm. Layers 1 and 4 consist of a single 30% square. Layers 2 and 3 are single 60%.

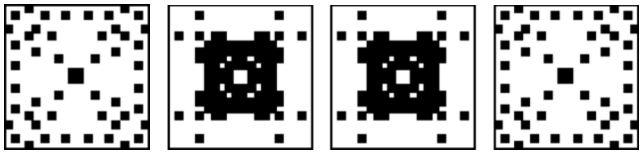

Fig 9 The best solution from stage 2 for the fifth order Butterworth low pass filter example. These are the 4-fold 20x20 binary patterns settled on for the four layers.

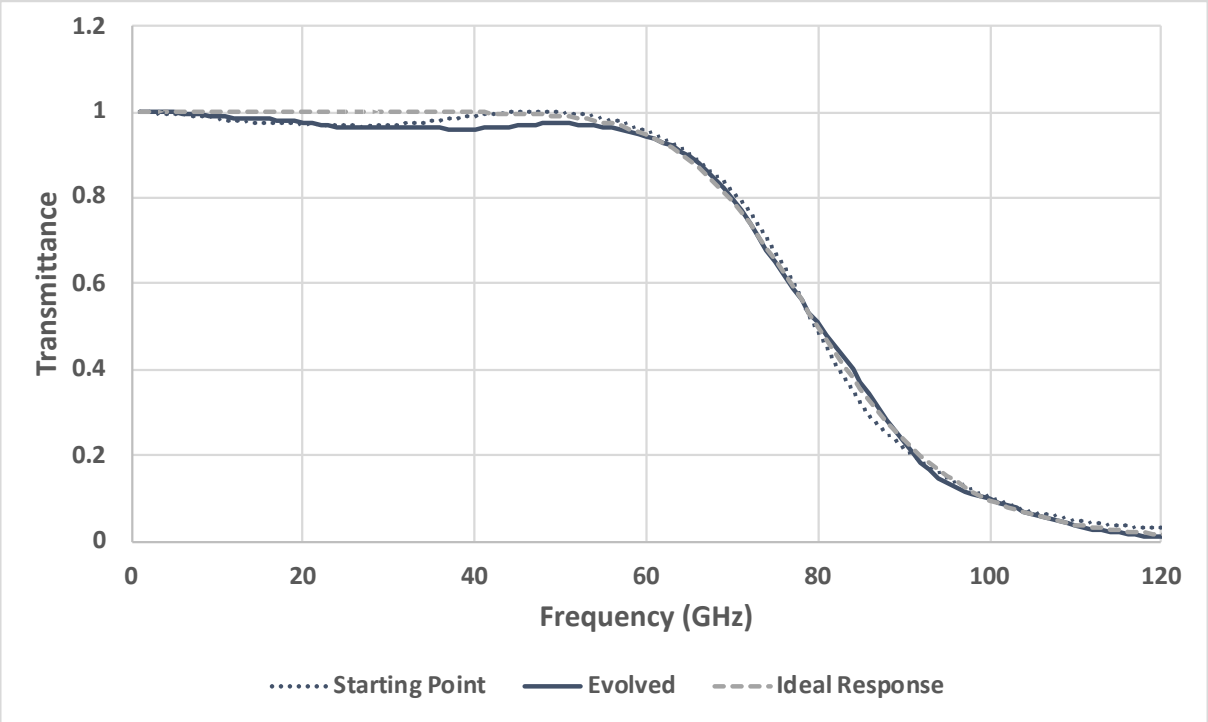

Fig 10 The best solution from stage 2 for the fifth order Butterworth low pass filter example. These are the 4-fold 20x20 binary patterns settled on for the four layers.

Chebyshev filter, three quarters of this comes about through a better conformance to the roll off on the approach to the stop band, arguably an unimportant improvement.

The losses incurred by the signal passing through the filter were again estimated, shown in Fig. 11. The losses for both the capacitive squares pattern produced by stage 1 and the binary pattern produced by stage 2 are very similar and minimal up to the 125GHz search limit.

4.3 An existing filter

A six layer mesh filter design that has been used on a number of millimeter wave astronomy instruments, including the Atacama Cosmology Telescope,[25] was used to demonstrate the effects of the optimisation suggested. The original filter showed a Chebyshev-like response at the lower frequencies in its pass band. In accordance with the Chebyshev filter recommendation, the corners of the square patches used were cut off. The results of HFSS modelling is shown in Fig. 12. The

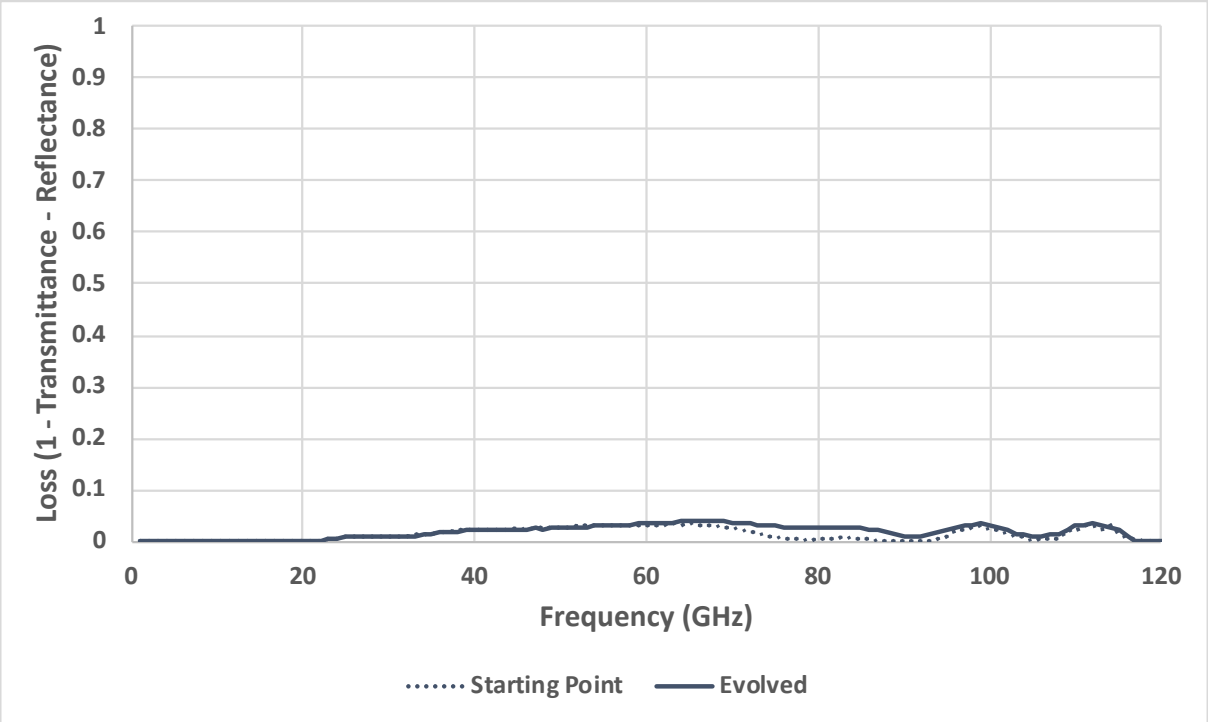

Fig 11 The losses of the starting point (the best solution from stage 1) and the best evolved solution from stage 2 for the Butterworth filter. The losses of the two solutions are minimal and very similar (the evolved pattern having a slightly higher loss around 80GHz) up to 125GHz limit of the search.

effect of removing the corners does reduce the pass band ripples slightly. In addition, the transition from pass band to the cut off is a little sharper. Both effects are quite small but may be useful.

5 Conclusions

The search for alternative shapes to conventional capacitive squares for the implementation of millimeter wave filters returned mixed results. The search concentrated on designs that conformed to a set of constraints to make their modelling possible. The aim, though, was to find shape changes that might be more generally applicable.

For Chebyshev-like filters, where ripple in the pass band is traded for a steeper cut-off, removing the corners from the conventional squares, can lead to a 35% improvement in the deviation from the theoretical transmittance. Most of this improvement is achieved in the pass band ripple

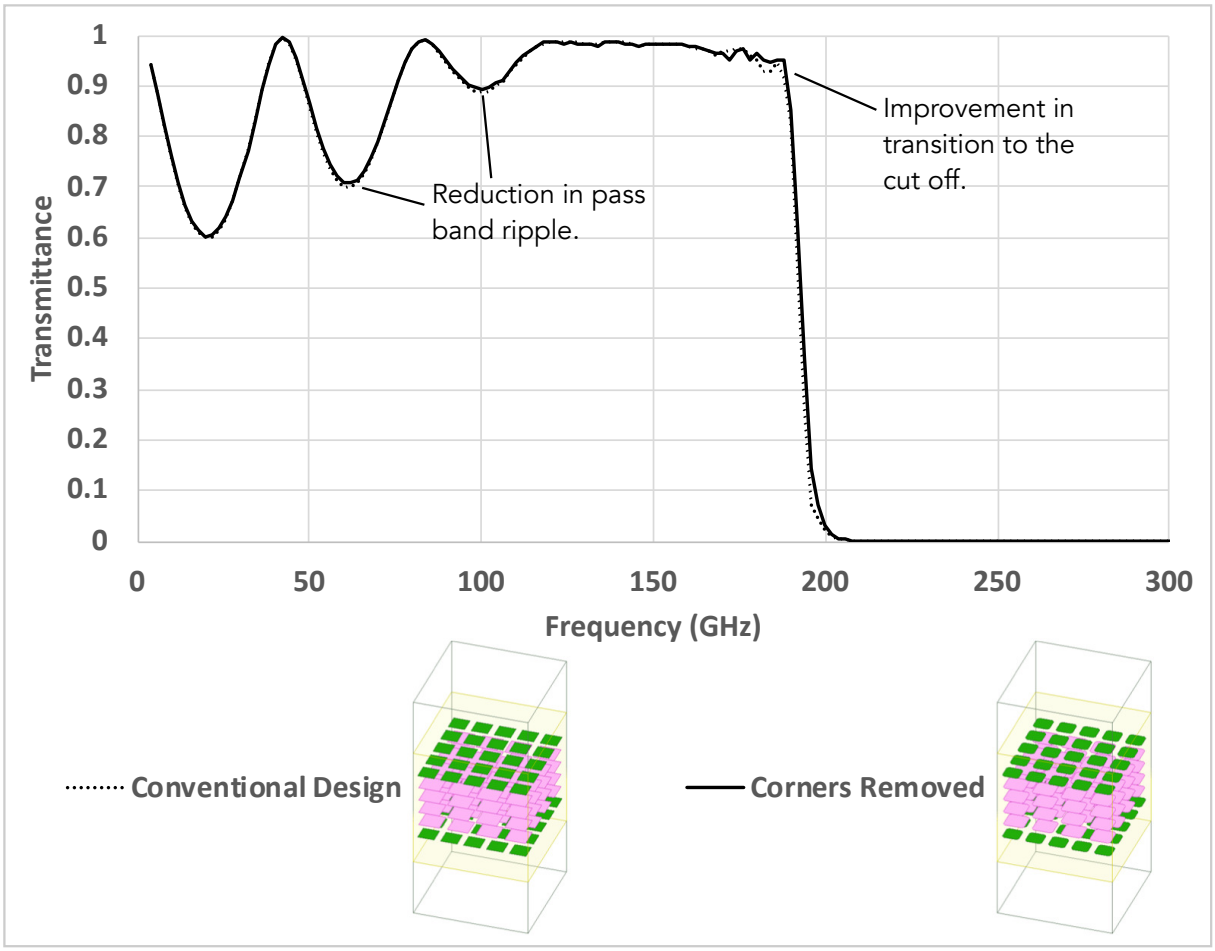

Fig 12 The response of a common low pass filter design used by the Cardiff group in various millimeter wave astronomy instruments showing the effect of removing the corners of the square patches.

which is significant. This can be achieved with minimal effect on losses. When applied to an existing filter, there was also a small sharpening of the pass band to cut off corner.

The Butterworth style filter tells a different story though. Although the evolved pattern in this case did show an 8% improvement in deviation from the theoretical transmittance curve, most of this improvement came about through better conformance of the cut-off near the stop band. A part of the curve where it can be argued small changes like this are not significant.

The experimental testing of the results reported was, unfortunately, halted due to the Covid-19 pandemic and remains outstanding for the foreseeable future. The modelling, manufacturing and testing of the mesh technology used in this study is well understood by the group at Cardiff and confidence is high that the performance of manufactured devices would be close to the modelling reported here. This has been demonstrated through a variety of conceptually different devices, half wave plates,[26,27] Toraldo pupils,[28] Magnetic mirrors,[29] Mesh lenses.[30,31]

Disclosures

The authors declare no conflicts of interest.

Acknowledgments

We acknowledge the support of the Supercomputing Wales project, which is part-funded by the European Regional Development Fund (ERDF) via Welsh Government.

References

1 R. Ulrich, "Far-infrared properties of metallic mesh and its complementary structure," *Infrared Physics* **7**, 37–55 (1967).

2 G. Pisano, C. Tucker, P. A. R. Ade, *et al.*, "Metal mesh based metamaterials for millimetre wave and THz astronomy applications," in *2015 8th UK, Europe, China Millimeter Waves and THz Technology Workshop (UCMMT)*, 1–4 (2015).

3 P. A. R. Ade, G. Pisano, C. Tucker, *et al.*, "A review of metal mesh filters," in *Millimeter and Submillimeter Detectors and Instrumentation for Astronomy III*, J. Zmuidzinas, W. S. Holland, S. Withington, *et al.*, Eds., SPIE, (Bellingham, WA) (2006).

4 M. Moallem and K. Sarabandi, "A single-layer metamaterial-based polarizer and bandpass frequency selective surface with an adjacent transmission zero," in *2011 IEEE International Symposium on Antennas and Propagation (APSURSI)*, 2649–2652 (2011).

5 Y. Wang, B. Yang, Y. Tian, *et al.*, "Micromachined Thick Mesh Filters for Millimeter-Wave and Terahertz Applications," *IEEE Transactions on Terahertz Science and Technology* **4**, 247–253 (2014).

6 A. M. Melo, A. L. Gobbi, M. H. O. Piazzetta, *et al.*, "Cross-Shaped Terahertz Metal Mesh Filters: Historical Review and Results," *Advances in Optical Technologies* **2012**, 530512 (2012).

7 M. Navarro-Cía, S. A. Kuznetsov, M. Aznabet, *et al.*, "Route for Bulk Millimeter Wave and Terahertz Metamaterial Design," *IEEE Journal of Quantum Electronics* **47**, 375–385 (2011).

8 A. Kundu, S. Das, S. Maity, *et al.*, "A tunable band-stop filter using a metamaterial structure and MEMS bridges on a silicon substrate," *Journal of Micromechanics and Microengineering* **22**, 045004 (2012).

9 T. Wu, "Novel metamaterial absorber with fractal elements," in *2015 IEEE International*

Symposium on Antennas and Propagation USNC/URSI National Radio Science Meeting, 244–245 (2015).

10 J. Holland, *Adaptation in Natural and Artificial Systems:An Introductory Analysis with Applications to Biology, Control, and Artificial Intelligence*, MIT Press (1992).

11 David E Goldberg, *Genetic algorithms in search, optimization and machine learning*, Addison-Wesley, Reading, Mass. (1988).

12 K. Krishnakumar, "Micro-Genetic Algorithms For Stationary And Non-Stationary Function Optimization," in *Intelligent Control and Adaptive Systems*, **1196**, 289–297, International Society for Optics and Photonics (1990).

13 Y. Ge and K. P. Esselle, "GA/FDTD technique for the design and optimisation of periodic metamaterials," *Antennas Propagation IET Microwaves* **1**, 158–164 (2007).

14 S. Sui, H. Ma, J. Wang, *et al.*, "Topology optimization design of a lightweight ultra-broadband wide-angle resistance frequency selective surface absorber," *Journal of Physics D: Applied Physics* **48**, 215101 (2015).

15 J. A. Thompson and G. Pisano, "Use of evolutionary computing algorithms in the design of millimetre-wave metamaterial devices," in *Millimeter, Submillimeter, and Far-Infrared Detectors and Instrumentation for Astronomy IX*, **10708**, 107083H, International Society for Optics and Photonics (2018).

16 P. Ranjan, A. Choubey, S. K. Mahto, *et al.*, "A six-band ultra-thin polarization-insensitive pixelated metamaterial absorber using a novel binary wind driven optimization algorithm," *Journal of Electromagnetic Waves and Applications* **32**, 2367–2385 (2018).

17 P. Ranjan, S. K. Mahto, and A. Choubey, "BWDO algorithm and its application in antenna

array and pixelated metasurface synthesis," *Antennas Propagation IET Microwaves* **13**(9), 1263–1270 (2019).

18 H. J. Mohammed, F. Abdulsalam, A. S. Abdulla, *et al.*, "Evaluation of genetic algorithms, particle swarm optimisation, and firefly algorithms in antenna design," in *2016 13th International Conference on Synthesis, Modeling, Analysis and Simulation Methods and Applications to Circuit Design (SMACD)*, 1–4 (2016).

19 S. D. Campbell, D. Sell, R. P. Jenkins, *et al.*, "Review of numerical optimization techniques for meta-device design [Invited]," *Optical Materials Express* **9**, 1842–1863 (2019).

20 S. Orfanidis, "Electromagnetic Waves and Antennas." 2016 (accessed 7 November 2017) [http://www.ece.rutgers.edu/~orfanidi/ewa/].

21 A. Taflove and S. C. Hagness, *Computational electrodynamics : the finite-difference time-domain method*, Artech House (2005).

22 J. B. Schneider, "Understanding the Finite-Difference Time-Domain Method." 2010 (accessed 23 March 2020) [www.eecs.wsu.edu/~schneidj/ufdtd].

23 S.-W. Lee, G. Zarrillo, and C.-L. Law, "Simple formulas for transmission through periodic metal grids or plates," *IEEE Transactions on Antennas and Propagation* **30**, 904–909 (1982).

24 "ANSYS HFSS: High Frequency Electromagnetic Field Simulation Software." (accessed 18 December 2019) [https://www.ansys.com/en-gb/products/electronics/ansys-hfss].

25 J. W. Fowler, M. D. Niemack, S. R. Dicker, *et al.*, "Optical design of the Atacama Cosmology Telescope and the Millimeter Bolometric Array Camera," *Applied Optics* **46**, 3444–3454 (2007).

26 G. Pisano, B. Maffei, P. A. R. Ade, *et al.*, "Multi-octave metamaterial reflective half-wave plate for millimeter and sub-millimeter wave applications," *Applied Optics* **55**, 10255–10262 (2016).

27 G. Pisano, B. Maffei, M. W. Ng, *et al.*, "Development of large radii half-wave plates for CMB satellite missions," in *Millimeter, Submillimeter, and Far-Infrared Detectors and Instrumentation for Astronomy VII*, **9153**, 915317, International Society for Optics and Photonics (2014).

28 G. Pisano, A. Shitvov, C. Tucker, *et al.*, "Metamaterial-based Toraldo pupils for super-resolution at millimetre wavelengths," in *Millimeter, Submillimeter, and Far-Infrared Detectors and Instrumentation for Astronomy IX*, **10708**, 107080G, International Society for Optics and Photonics (2018).

29 G. Pisano, P. A. R. Ade, and C. Tucker, "Experimental realization of an achromatic magnetic mirror based on metamaterials," *Applied Optics* **55**, 4814–4819 (2016).

30 G. Pisano, A. Shitvov, P. Moseley, *et al.*, "Development of large-diameter flat mesh-lenses for millimetre wave instrumentation," in *Millimeter, Submillimeter, and Far-Infrared Detectors and Instrumentation for Astronomy IX*, **10708**, 107080D, International Society for Optics and Photonics (2018).

31 G. Pisano, J. Austermann, J. Beall, *et al.*, "Development of Flat Silicon-Based Mesh Lens Arrays for Millimeter and Sub-millimeter Wave Astronomy," *Journal of Low Temperature Physics* **199**, 923–934 (2020).

Jonathan A. Thompson is a postgraduate student working towards a PhD in the School of Physics and Astronomy at Cardiff University, UK. His interests are in the use of meta-materials for the implementation of filters and lenses in the field of millimeter wave astronomy.

Giampaolo Pisano is a Reader in the School of Physics and Astronomy at Cardiff University, UK. His primary interest is new instrumentation focused on the detection of B-modes in the Cosmic Microwave Background. He has developed high performance RF devices such as phase shifters, orthomode transducers, polarizers and polarisation modulators along with novel quasi-optical components based on metamaterials such as mesh half-wave plates, mesh lenses and magnetic mirrors.

Carole Tucker is a Professor in the School of Physics and Astronomy at Cardiff University, UK. Her particular expertise lies with the quasi-optical filter technology for which Cardiff is the sole-provider worldwide. She has interests in the fields of FIR astronomical instrumentation for photometric and spectroscopic studies, Quasi Optics and metamaterials for FIR Astronomy and THz applications, IR to THz spectroscopy of optical components and materials and Cryogenic instrumentation.

List of Figures

3 The best solution from stage 1 for the seventh order Chebyshev low pass filter example. It consists of two layers repeated in reverse order with a repeat cell size of 1.716mm and a layer spacing of 0.875mm. Layers 1 and 4 consist of a 2x2 layout of 80% squares each in a unit cell of 0.858mm. Layers 2 and 3 are single 70% squares in a unit cell of 1.716mm covering the entire repeat cell.

4 The best solution from stage 2 for the seventh order Chebyshev low pass filter example. These are the 4-fold 20x20 binary patterns settled on for the four layers.

5 The transmittance curves of the starting point (the best solution from stage 1), the best evolved solution from stage 2 and the ideal filter response. It can be seen that the plate pattern changes from the stage 2 evolution have caused the transmittance characteristic to move closer to the target; most significantly, the pass-band ripple has been reduced.

6 The losses of the starting point (the best solution from stage 1) and the best evolved solution from stage 2 for the Chebyshev filter. The losses of the two solutions are minimal and similar within the passband. In the stop band, however, the evolved solution showed significant loss around 125GHz. The diffraction limit is at 160GHz.

7 Fitness factors were calculated for the result of stage 2 and for patterns with various stage 2 changes removed. The conclusion is that the corners of layers 2&3 and the outer corners of layers 1&4 make the most difference. The other changes appear to make only a marginal difference.

8 The best solution from stage 1 for the fifth order Butterworth low pass filter example. It consists of two layers repeated in reverse order with a repeat cell size of 1.789mm and a layer spacing of 1.167mm. Layers 1 and 4 consist of a single 30% square. Layers 2 and 3 are single 60%.

9 The best solution from stage 2 for the fifth order Butterworth low pass filter example. These are the 4-fold 20x20 binary patterns settled on for the four layers.

10 The best solution from stage 2 for the fifth order Butterworth low pass filter example. These are the 4-fold 20x20 binary patterns settled on for the four layers.

11 The losses of the starting point (the best solution from stage 1) and the best evolved solution from stage 2 for the Butterworth filter. The losses of the two solutions are minimal and very similar (the evolved pattern having a slightly higher loss around 80GHz) up to 125GHz limit of the search.

12 The response of a common low pass filter design used by the Cardiff group in various millimeter wave astronomy instruments showing the effect of removing the corners of the square patches.